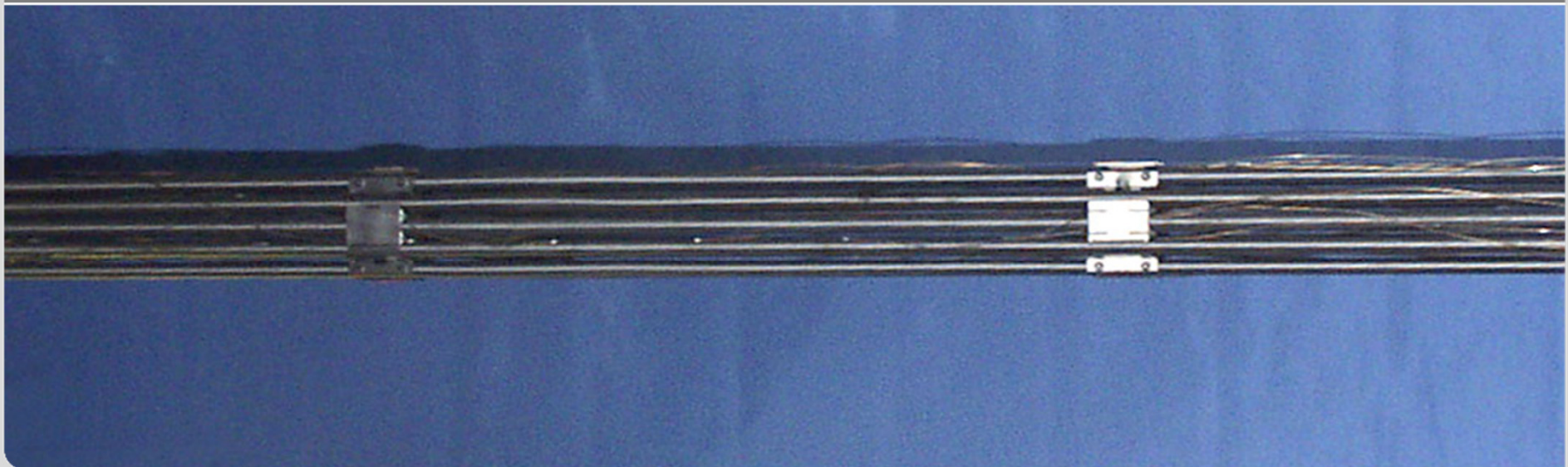


Influence of the Temperature History on Secondary Hydriding and Mechanical Properties of Zircaloy-4 Claddings - an Analysis of the QUENCH-LOCA Bundle Tests

J. Stuckert, M. Große, C. Rössger, M. Steinbrück, M. Walter

Paper ICONE22-30792

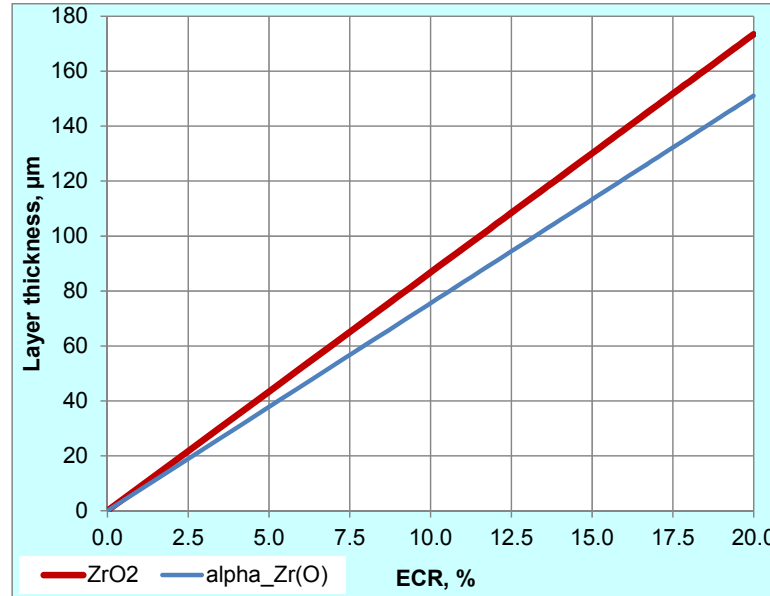
Institute for Applied Materials; Program NUKLEAR



Embrittlement due to oxidation



1250 K
 outer ZrO₂ 100 μm; α-Zr(O) 70 μm;
 inner ZrO₂ 30 μm; α-Zr(O) 80 μm



Cathcart - Pawel kinetics



Equivalent Cladding Reacted

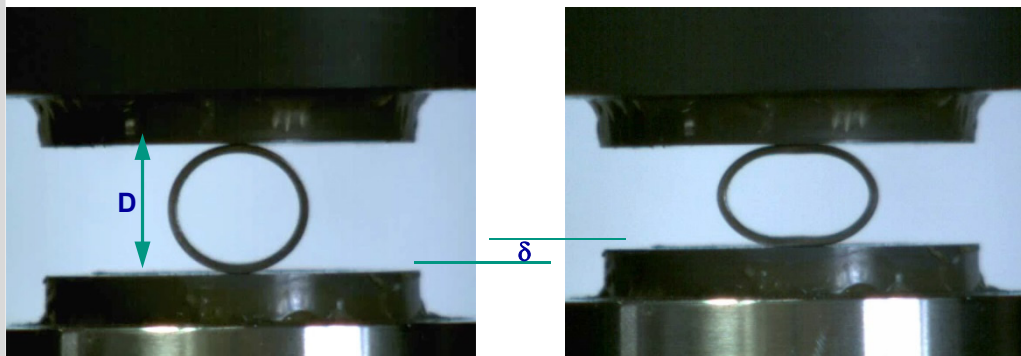
$$ECR = \frac{(m_{O_2}/MO_2)}{\frac{(\tau_{cl} \cdot \rho_{Zr})}{M_{Zr}}}$$

m_{O_2} - oxygen in
 1 cm² clad [g/cm²]

τ_{cl} - initial clad
 thickness [cm]

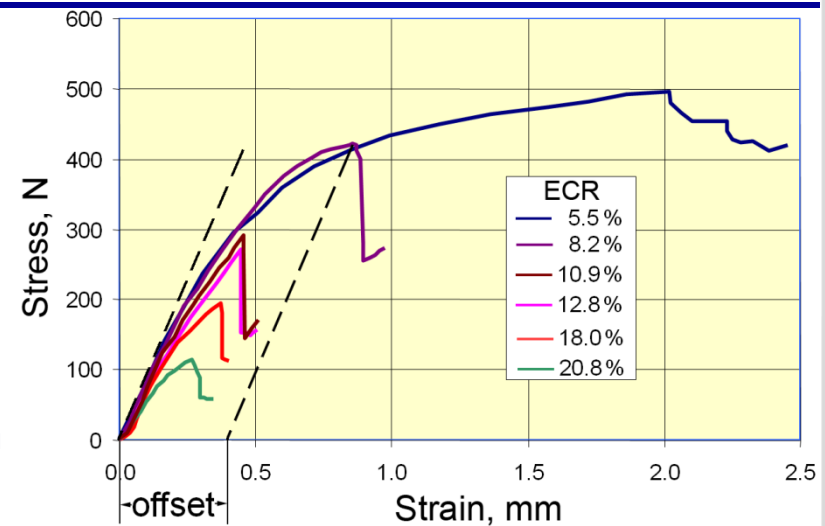
ρ - density [g/cm³]

M - molar mass [g/mol]

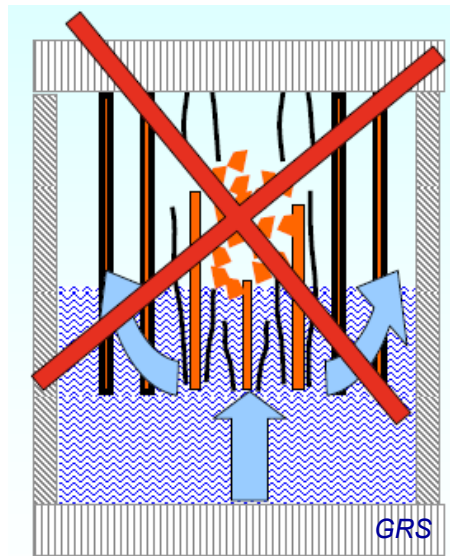
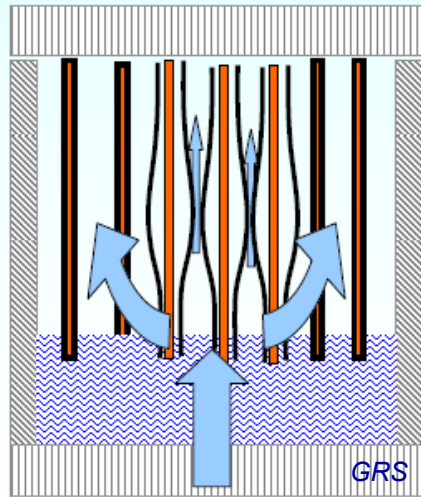


ANL ring compression tests: Embrittlement occurs when permanent plastic deformation (offset strain) $\delta/D < 2\%$, i.e. $\delta \lesssim 0.2$ mm

US NRC, 1973: ECR ≤ 17%
 and peak cladding T < 1200°C



Present Regulatory Limit for LOCA (international)



Maintain coolable geometry



Keep fuel inside cladding



Prevent breaking cladding



Maintain residual ductility in cladding



Limit oxidation



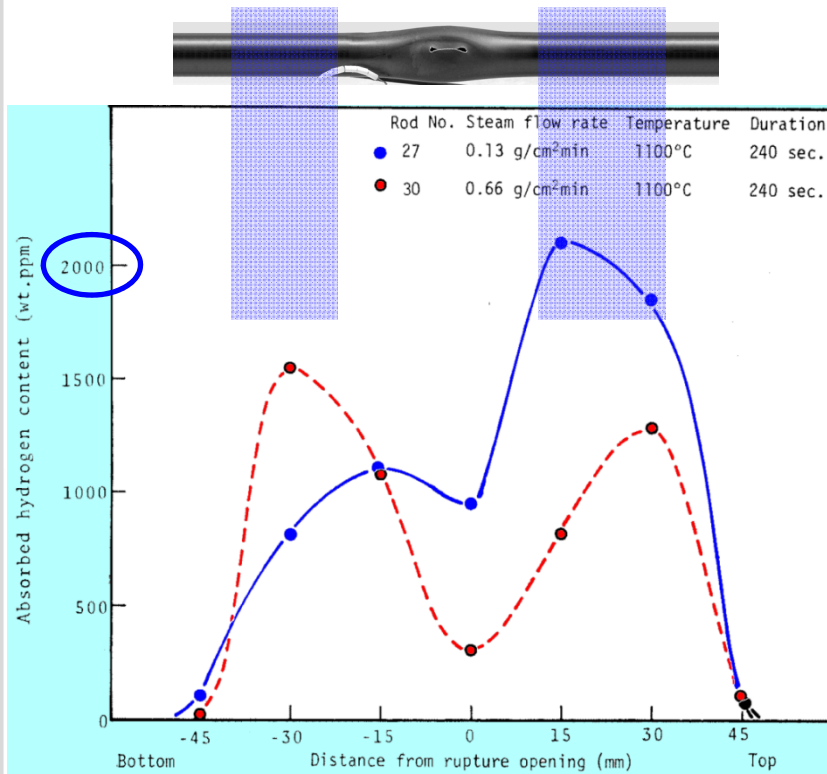
(Limit hydriding - under consideration)

- Oxidation limits
 - Keep equivalent cladding reacted below 17% → **ECR** < 17%
 - Keep oxidation temperature below 1200°C → **PCT** < 1200°C
 - **Keep hydriding below ?** → **ECR = ECR(H)**

Secondary hydriding:

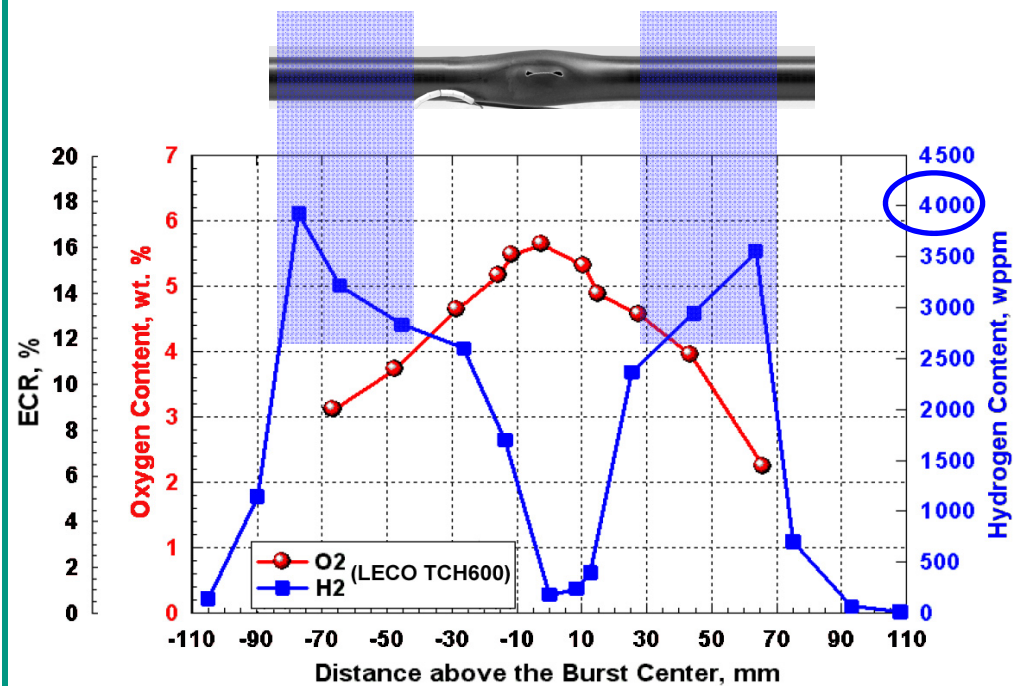
Hydrogen peaks above and below burst openings

1981, JAERI*: first observation of cladding hydriding by steam ingress through the burst opening at 1100°C



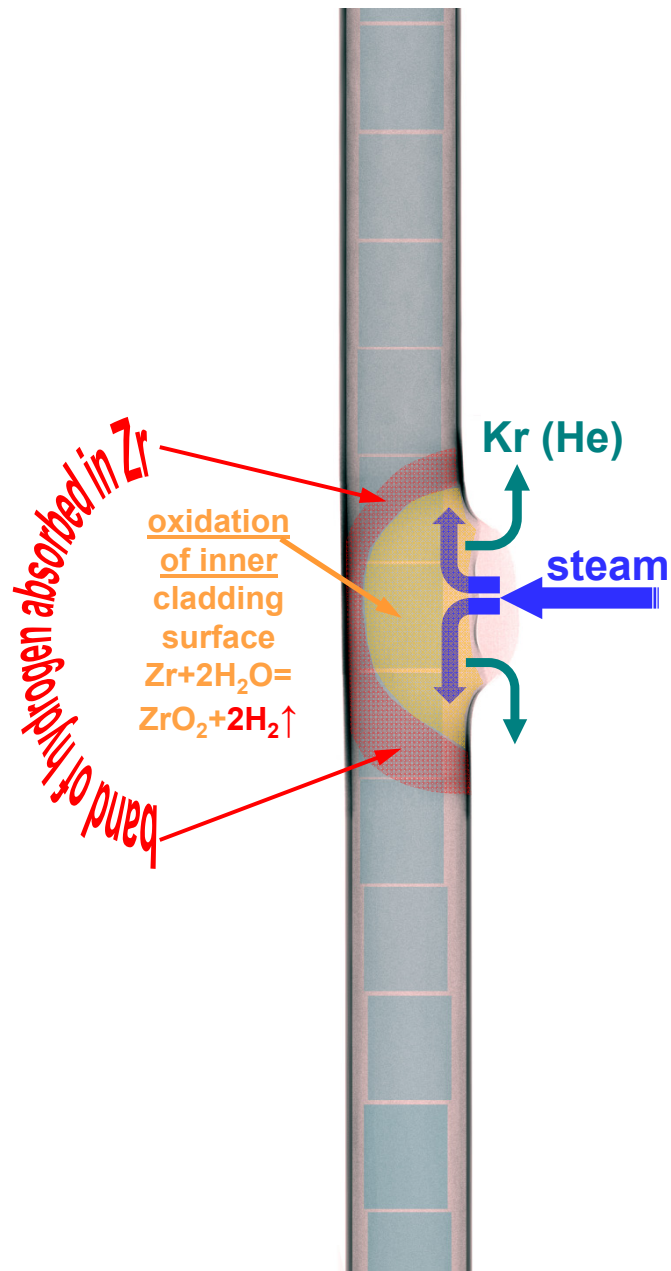
Uetsuka et al., Journal of NUCLEAR SCIENCE and TECHNOLOGY, 18[9], pp. 705~717 (September 1981).

2008, ANL: strong hydriding at 1200°C up to 4000 wppm



NUREG-6967 (Billone et al.): unirradiated pressurised sample OCL11 (Zry-2) ramped in steam from 300°C to 1204°C at 5 K/s, held at 1204°C for 300 s, cooled at 3 K/s to 800°C, and cooled from 800°C to RT

Mechanism of secondary hydrogenation of cladding



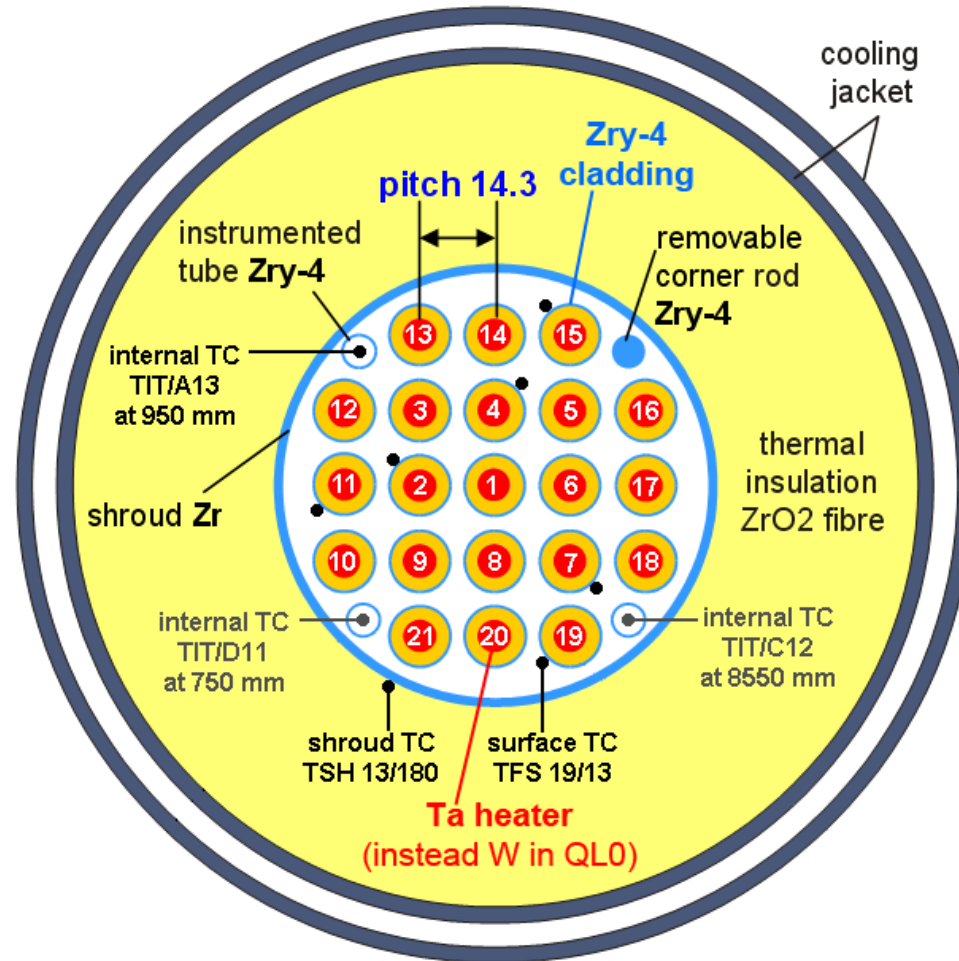
Sequence of phenomena:

- cladding ballooning and burst, relief of inner rod pressure
- steam penetration through the burst opening, steam propagation in decreasing gap between cladding and pellet
- oxidation of inner cladding surface with hydrogen release
- absorption of hydrogen by cladding at the boundary of inner oxidised area
- local embrittlement of cladding near to burst opening

Objective for new LOCA bundle tests

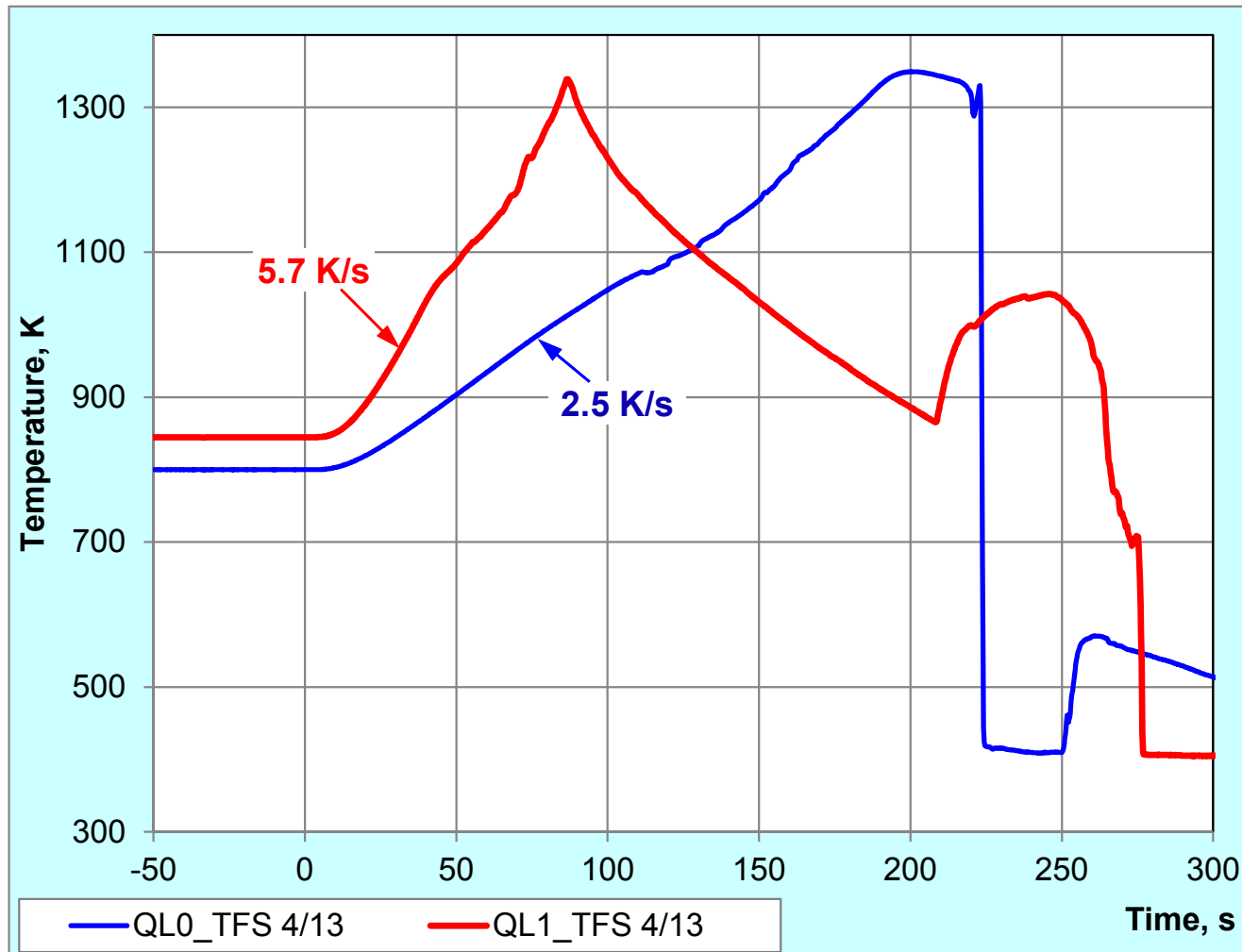
- Higher burn-up: increased oxidation during normal operation and pertaining hydrogen uptake
- Secondary hydriding of cladding after burst
- Application of new cladding alloys
- Evidence of core coolability
- Contribution to modification of current LOCA embrittlement criteria (1200°C, 17% ECR) with consideration of cladding hydrogenation

Cross-section of the QUENCH-L1 bundle



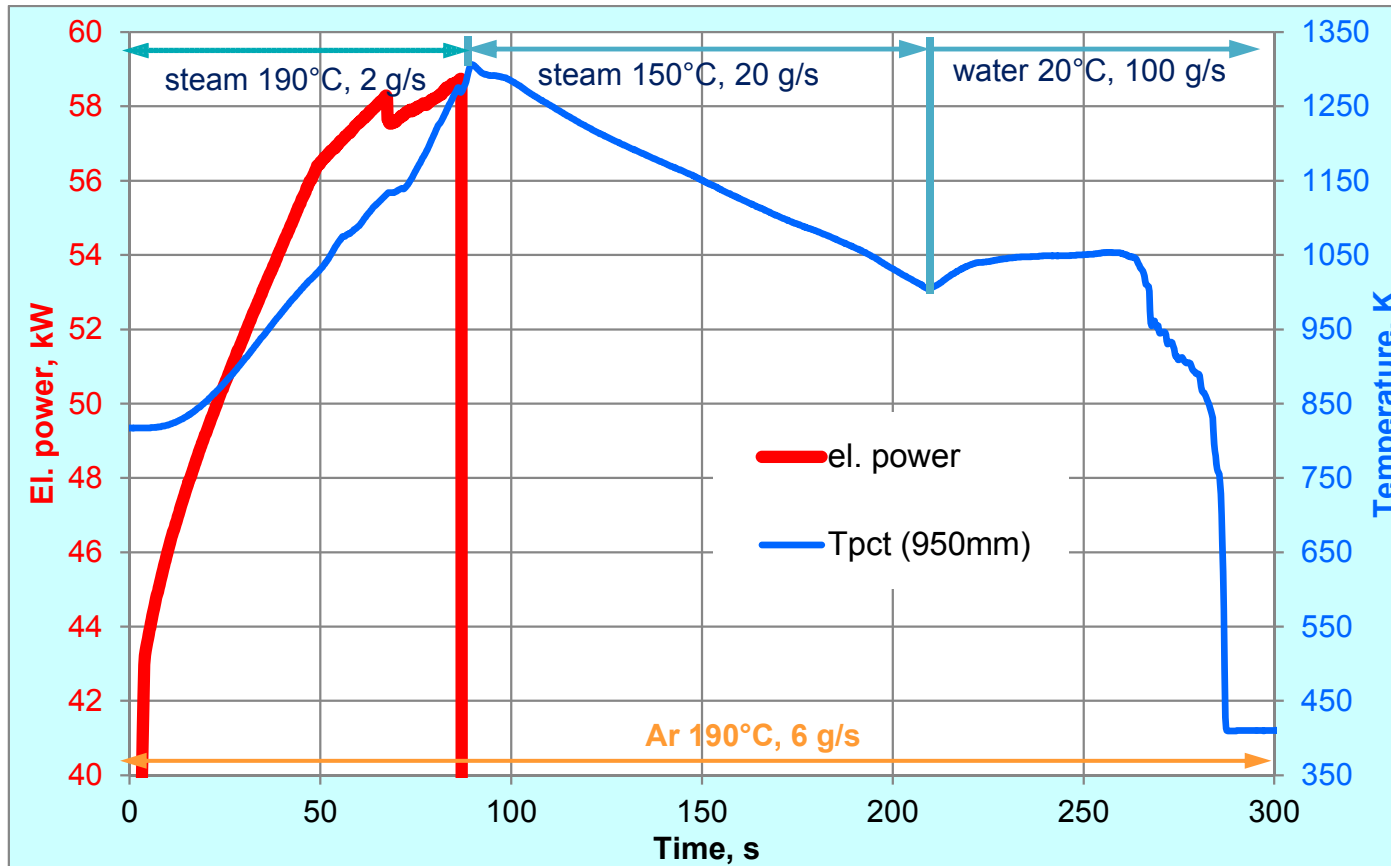
all rods filled with Kr at $p = 55$ bar
and $T_{pct} = 800$ K

Comparison of cladding temperatures at hottest bundle elevation of 950 mm for QUENCH-L0 and -L1



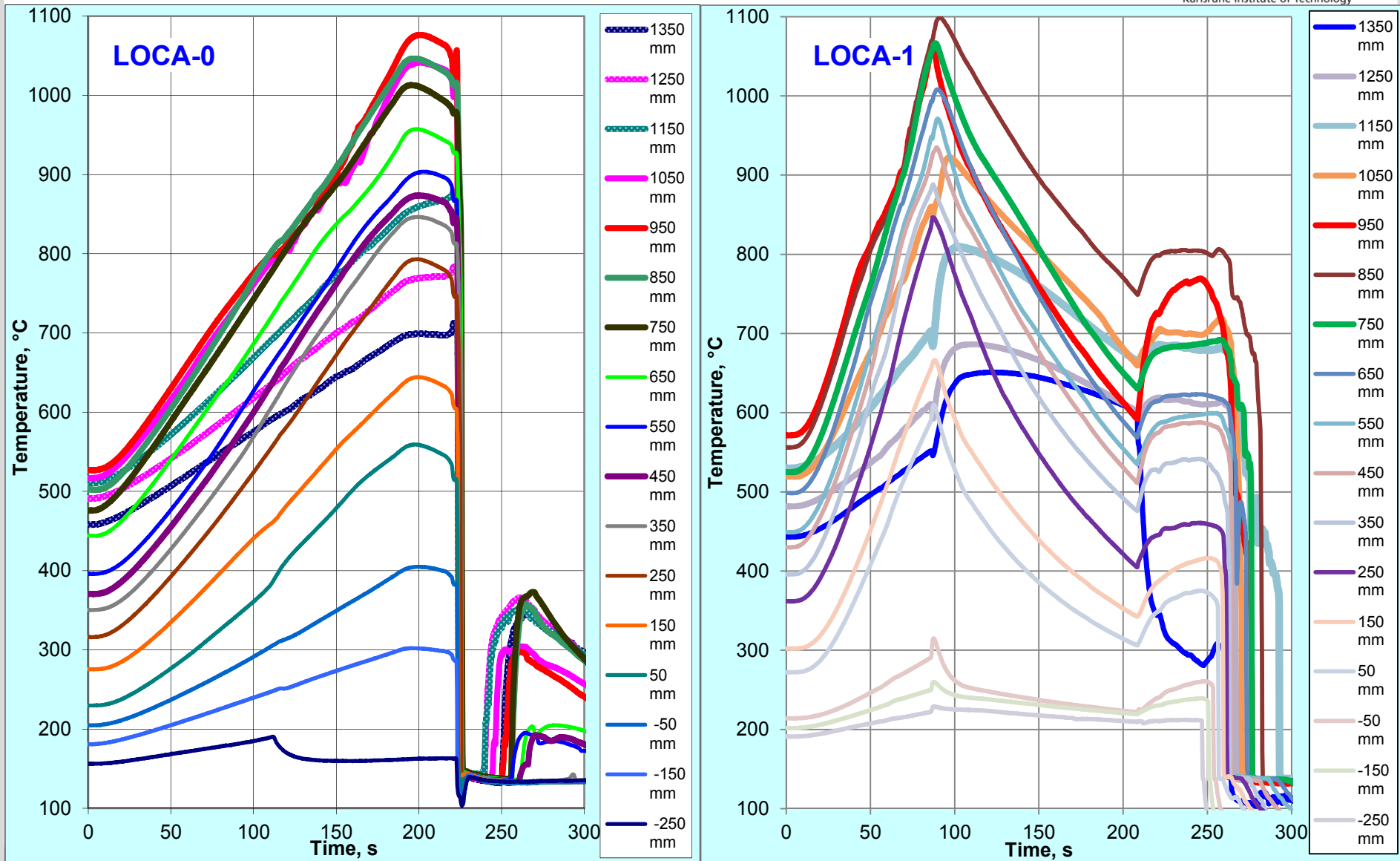
enhancements for QUENCH-L1:
1) prototypical high heating rate; 2) prototypical cool-down phase

Progress and boundary conditions of the QUENCH-L1 test

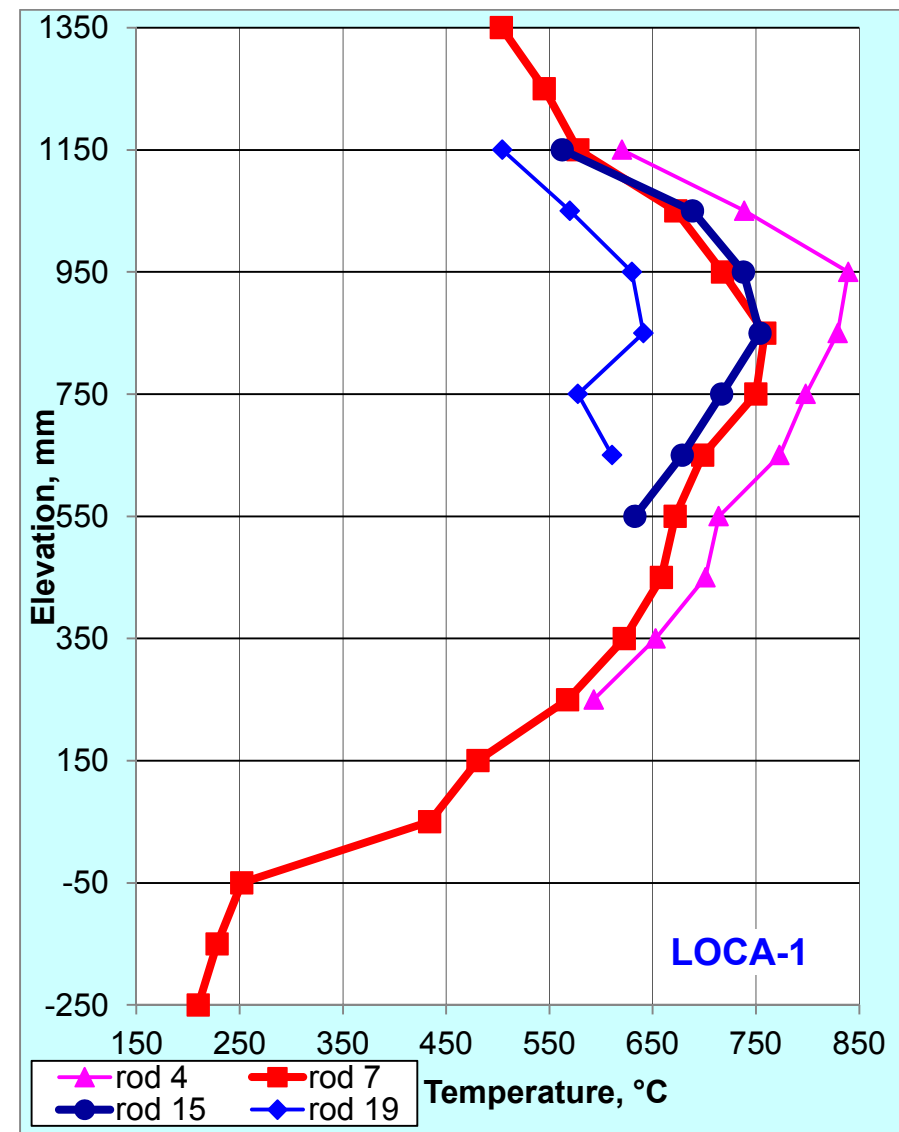
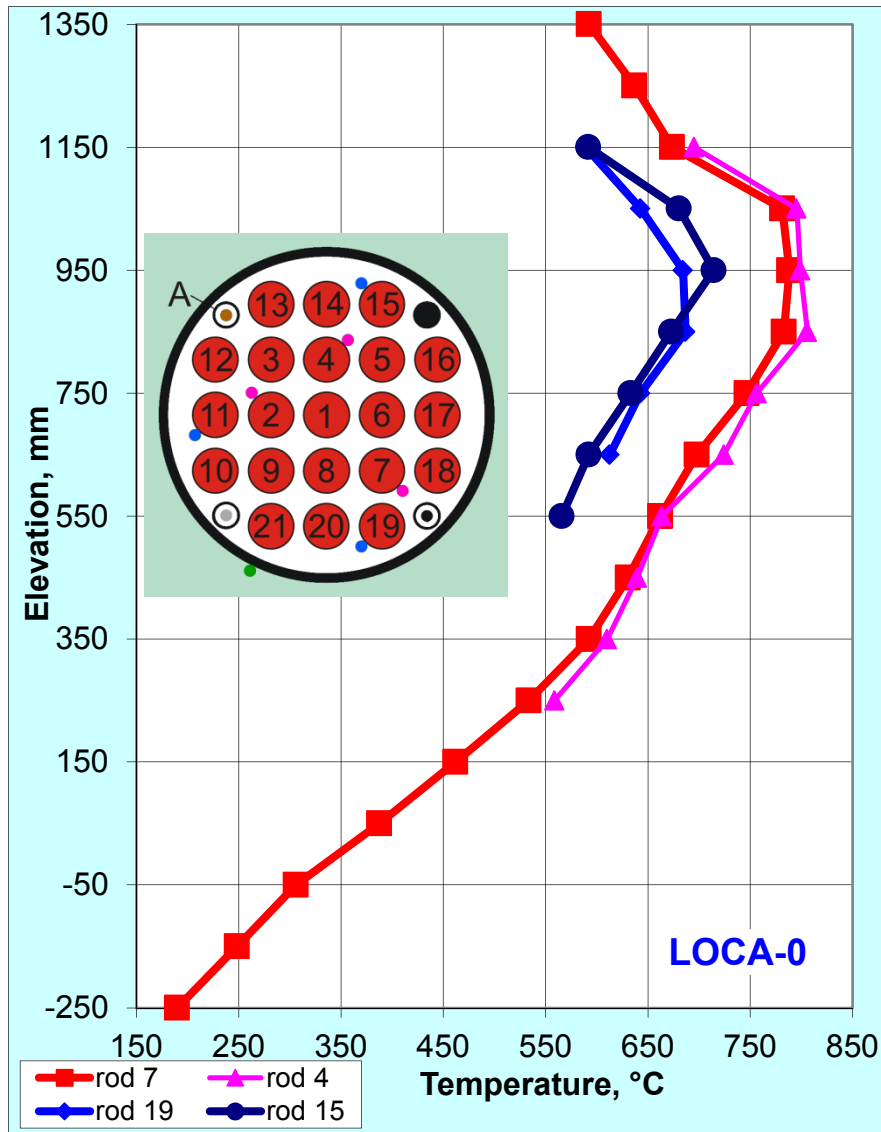


maximal reached power:
QUENCH-L1 (Ta-heaters, Ø 6 mm): 58.5 kW,
QUENCH-L0 (W-heaters; Ø 6 mm): 43 kW

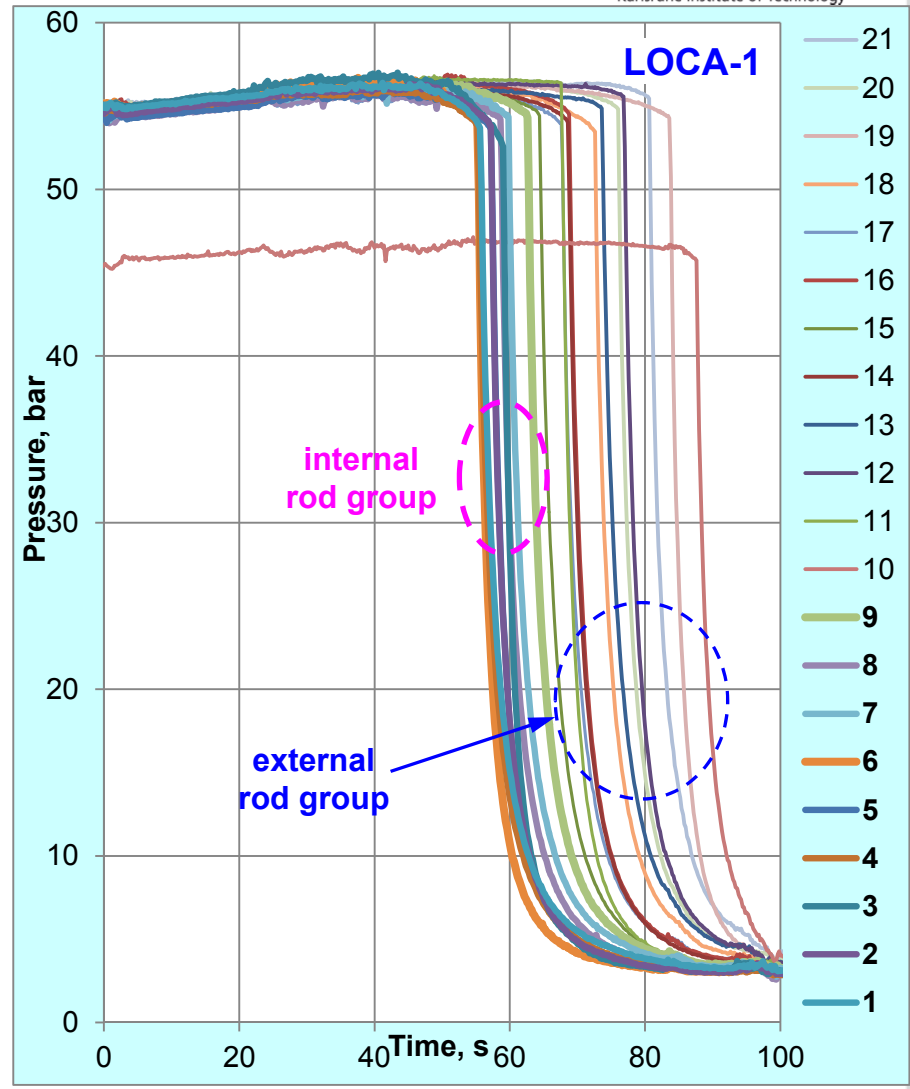
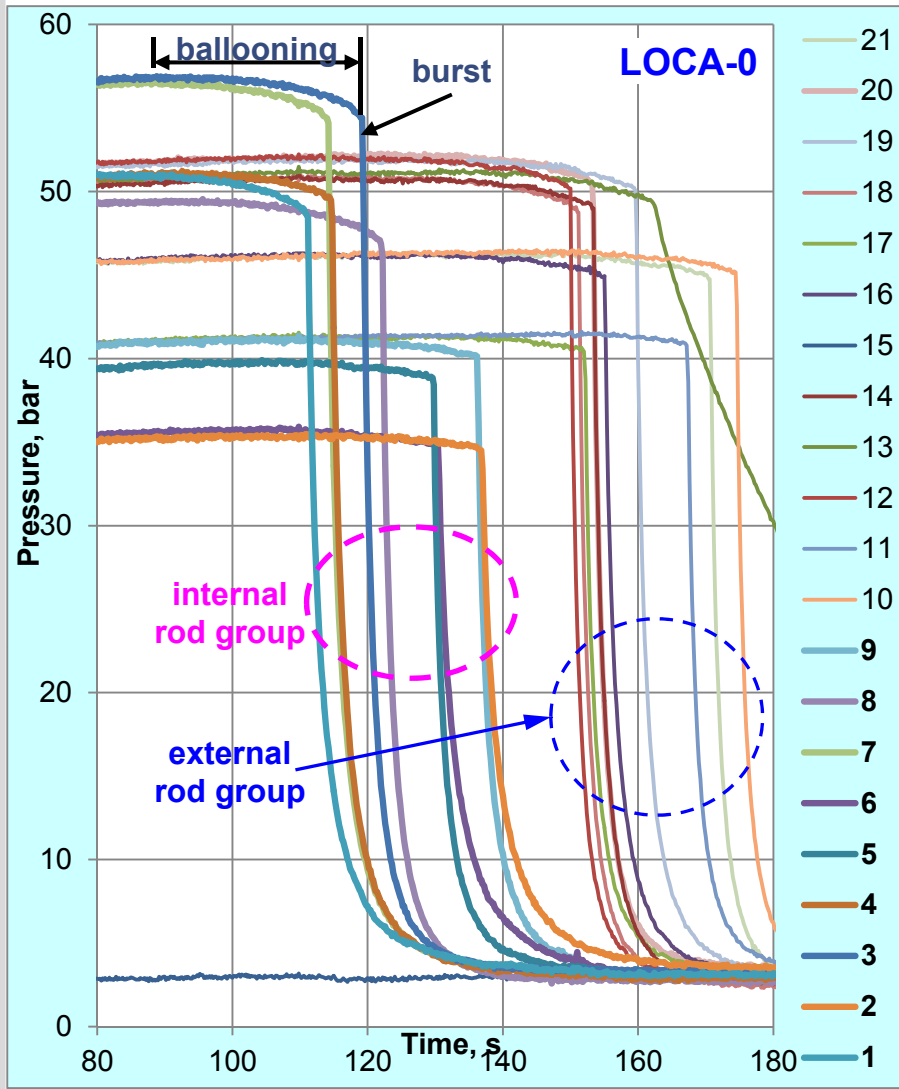
Comparison of maximal cladding temperatures at different elevations for QUENCH-L0 and -L1



Axial and radial temperature distributions at first burst for QUENCH-L0 (111 s, rod #1) and -L1 (55 s, rod #4)

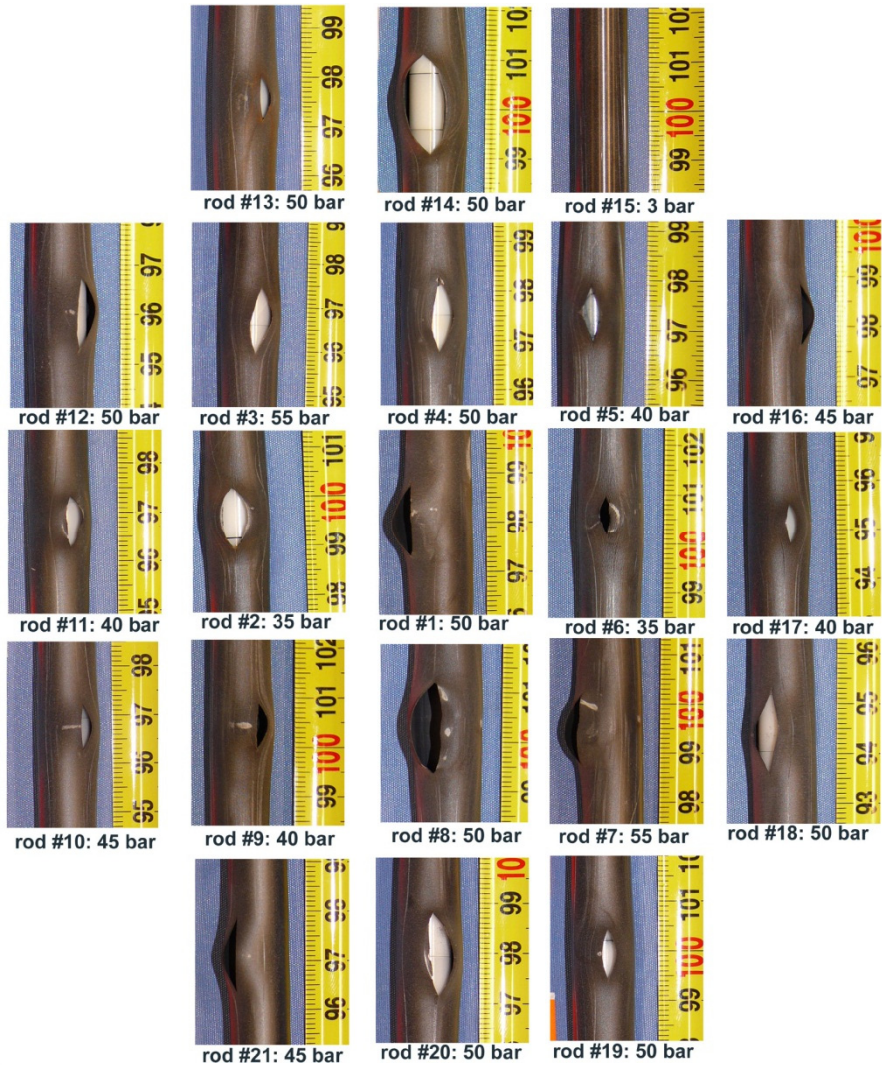


Rod pressure evolution during heating phase for QUENCH-L0 and -L1: burst time indication (coincided with MS results on Kr release)

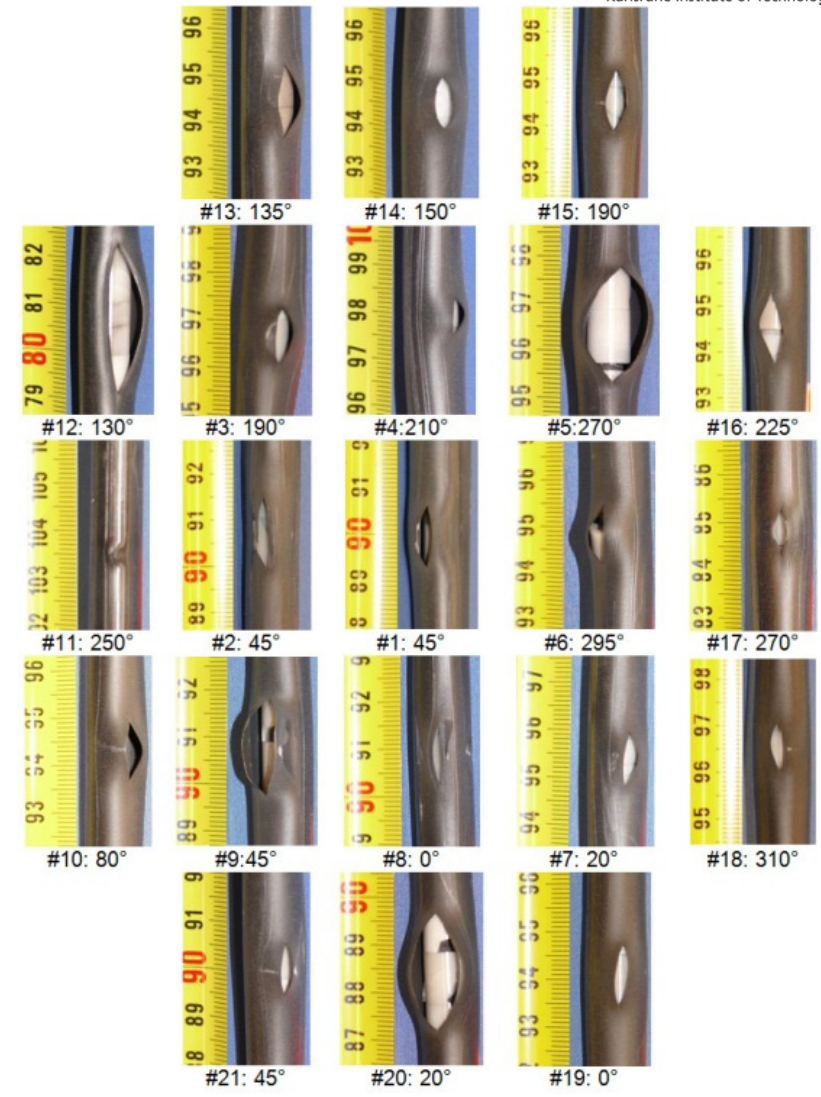


duration of decrease of the inner pressure to the system pressure: $\tau_0 \approx 38$ s

Overview of burst openings

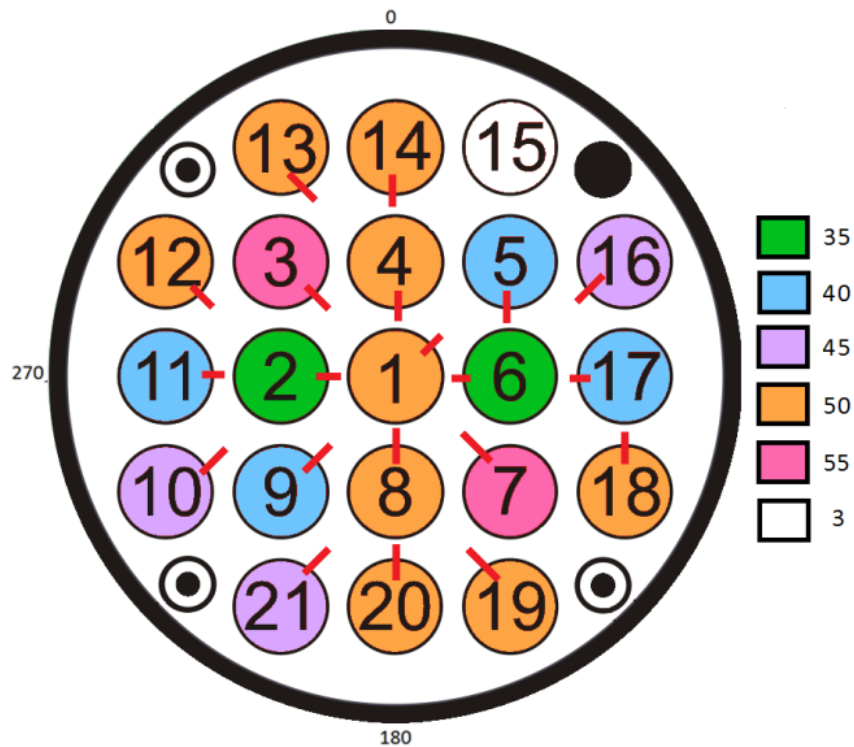


LOCA-0

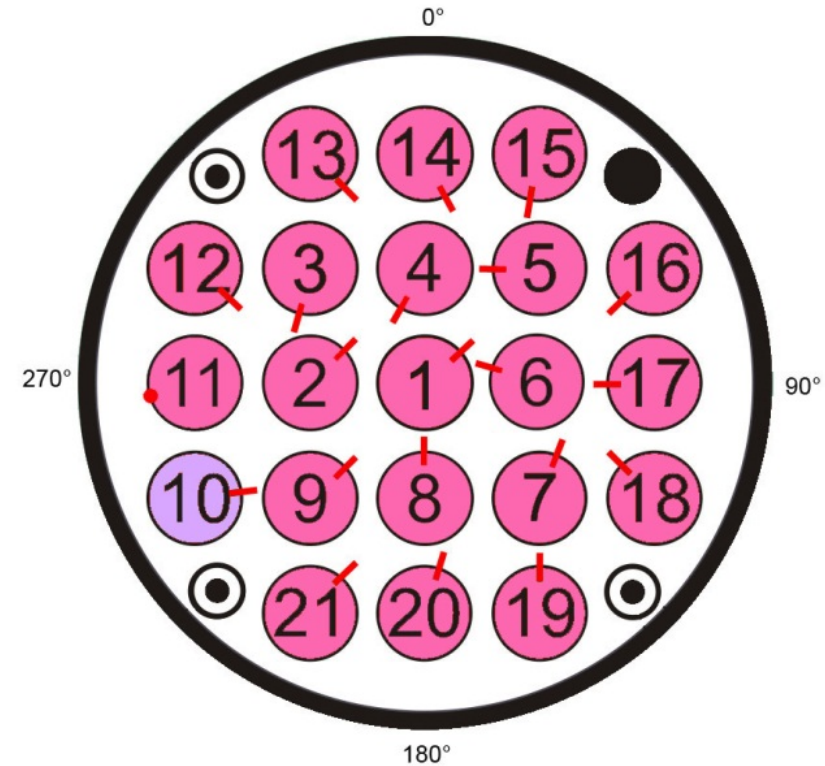


LOCA-1

Circumferential positions of burst openings



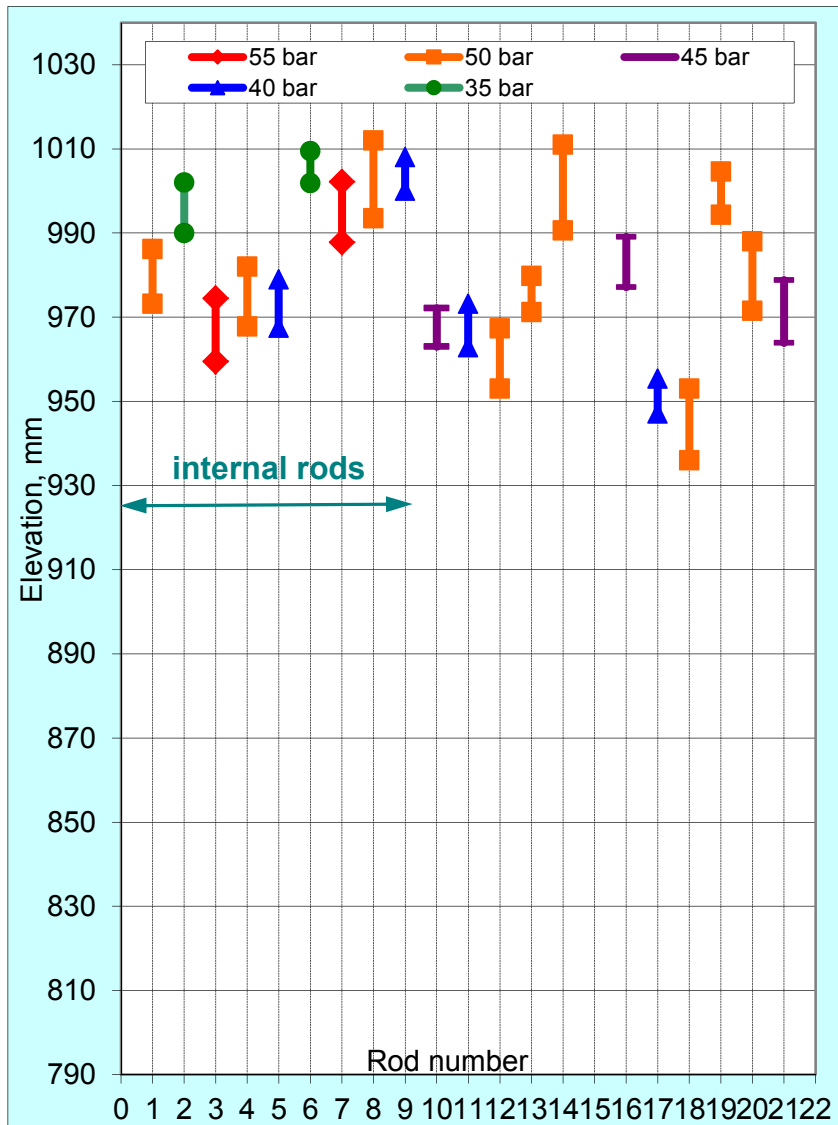
LOCA-0:
 openings oriented
 to bundle center
 due to strong radial T gradient



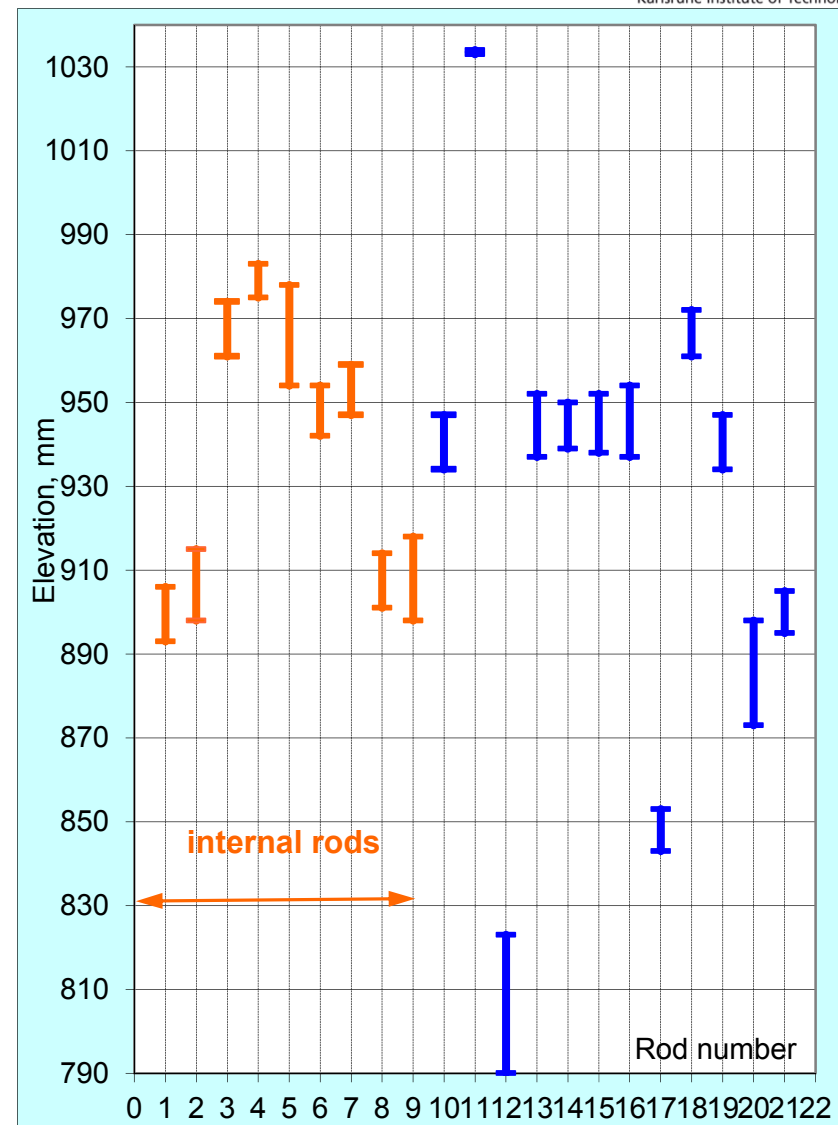
LOCA-1:
 less pronounced orientation
 to bundle center

Length and axial position of burst openings

LOCA-0



LOCA-1



Burst-Parameters

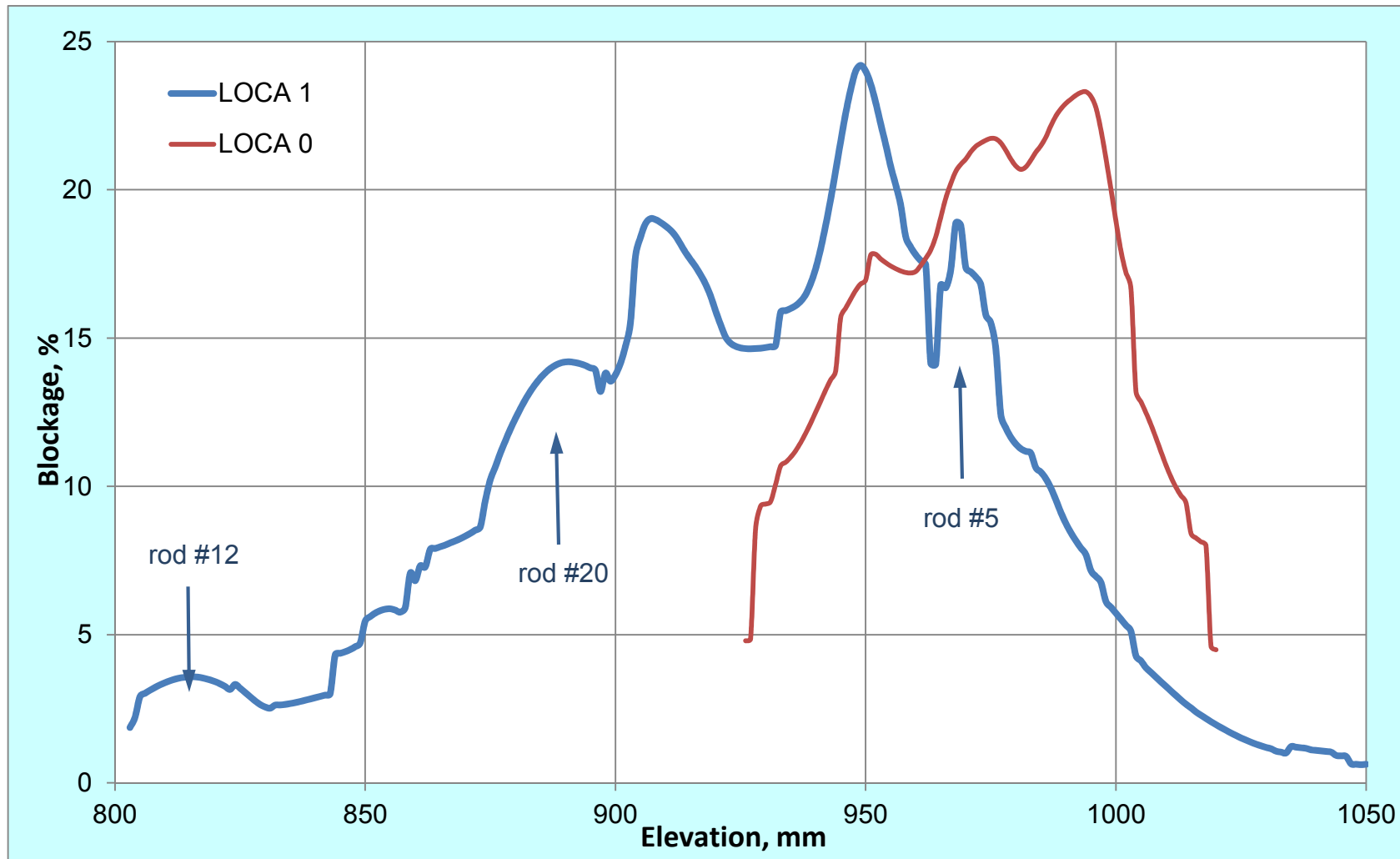
LOCA-0 (transient ca. 220 s)

Rod group	Rod #	Burst time, s	Burst temperature, interpolated, °C
Center	1	111.2	914
	7	114.2	888
	4	114.6	867
	3	119.2	881
	8	122.0	880
	5	129.6	911
	6	130.4	910
	9	136.2	939
	2	136.8	940
	Periphery	12	150.0
18		151.2	907
17		152.0	933
20		153.2	849 (Min)
14		153.4	898
16		155.0	894
19		159.6	929
13		162.5	880
11		167.2	948 (Max)
21		170.6	870
10		174.4	865

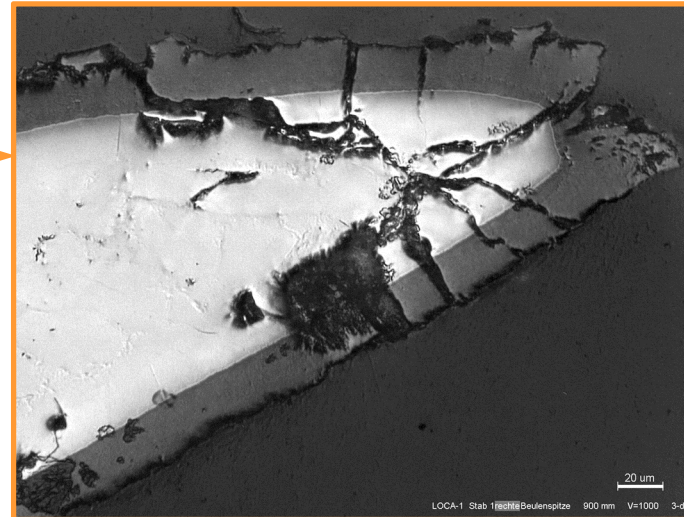
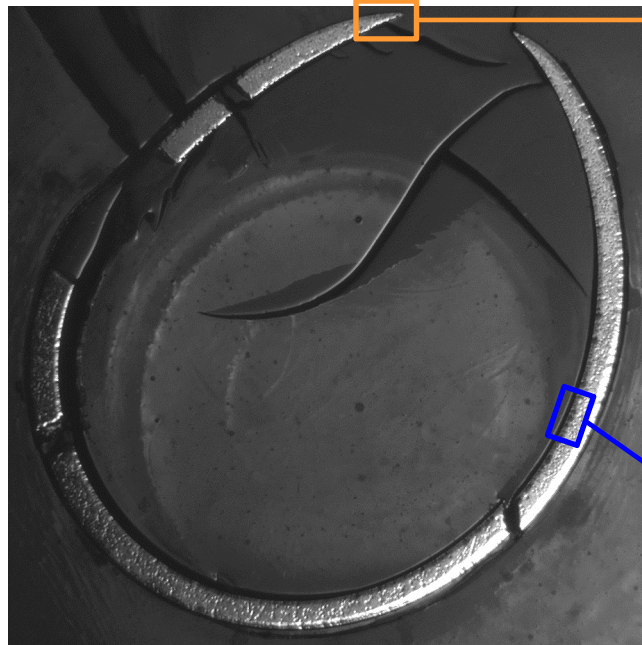
LOCA-1 (transient ca. 80 s)

Rod group	Rod #	Burst time, s	Burst temperature, interpolated, °C
Zentralstäbe	4	55.2	881
	6	55.2	837
	1	55.6	896 (Max)
	5	57.2	831
	2	57.2	859
	8	58.6	859
	3	59.0	845
	7	59.8	801 (Min)
	9	62.6	889
	Peripheriestäbe	15	64.4
17		67.6	831
11		67.6	783
14		68.6	881
16		68.8	883
18		72.6	808
13		73.6	874
20		76.0	832
12		76.8	819
21		80.6	867
19		83.6	890
10		87.6	870

Cooling channel blockage for LOCA-0 and LOCA-1



Outer and inner cladding oxidation at 900 mm for LOCA-1, rod #1

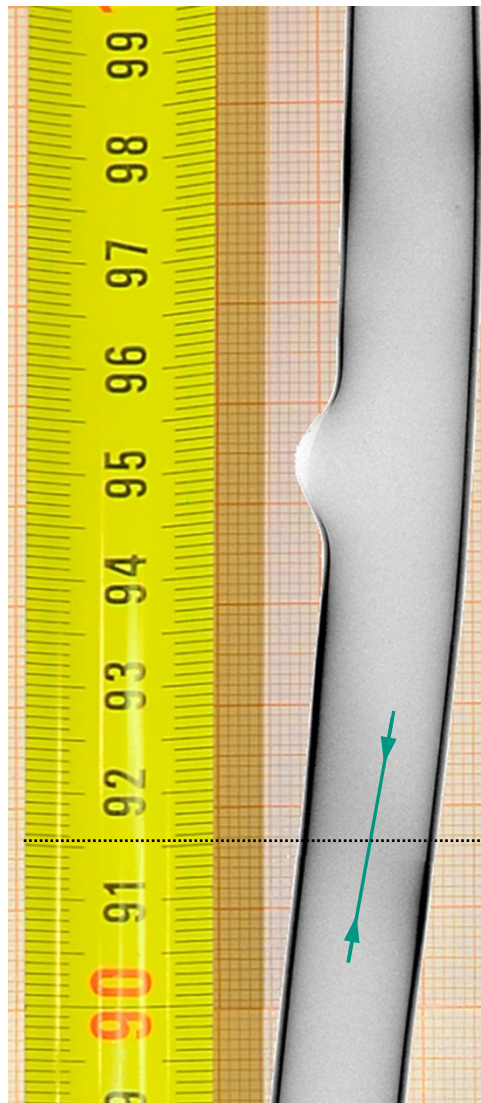


inner and outer oxide
layer thickness:
20 µm

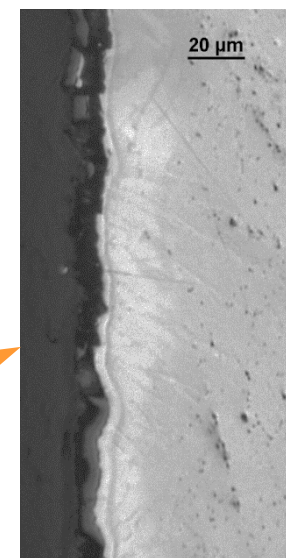
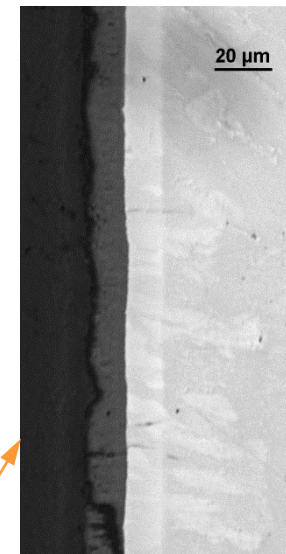
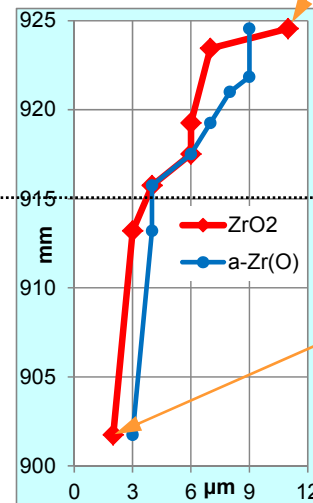


inner oxide:
layer thickness:
20 µm

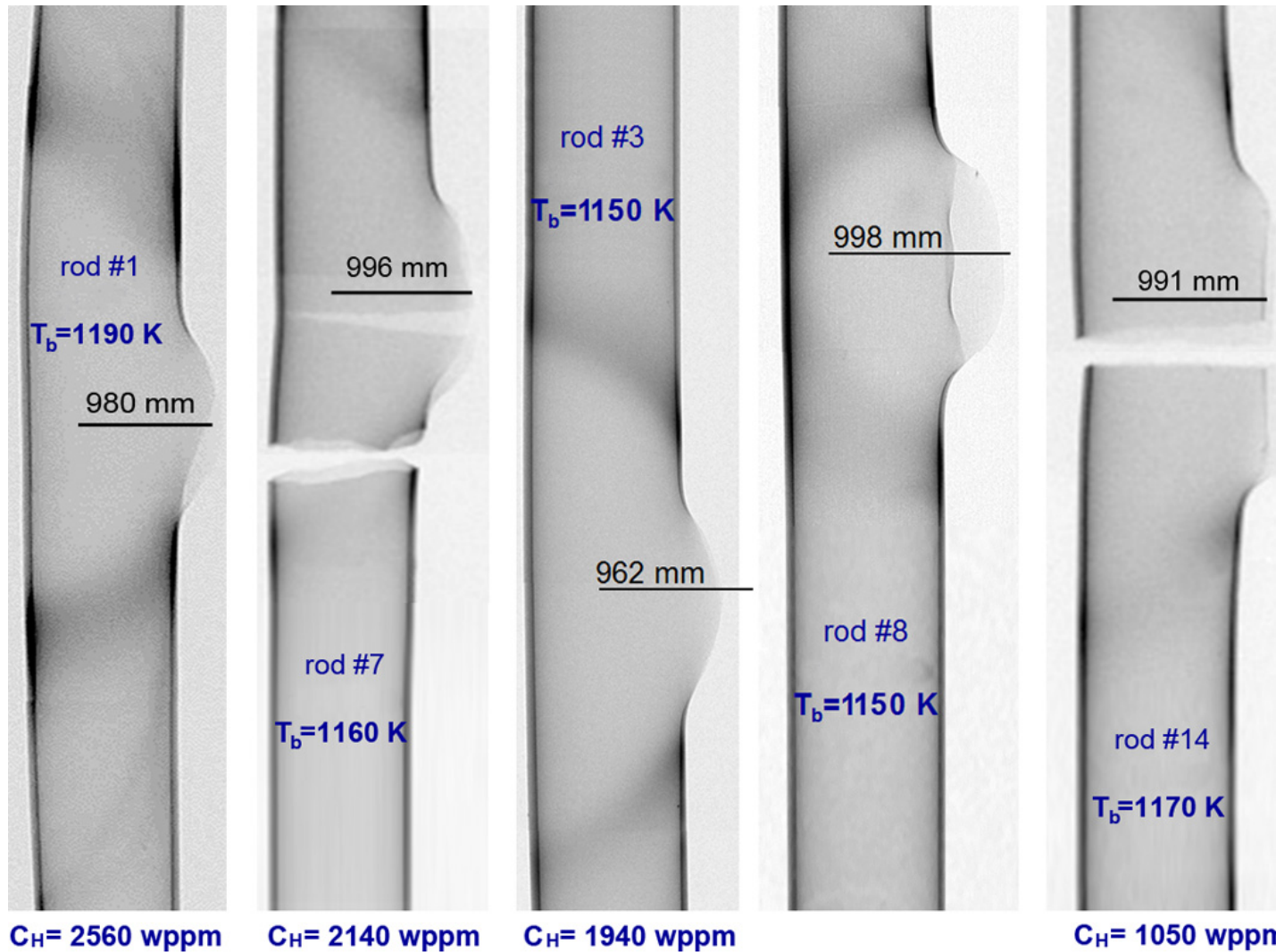
QL1, rod #6: axial distribution of inner oxidation in region of secondary hydrogenation



metallographic measurements along longitudinal cut:



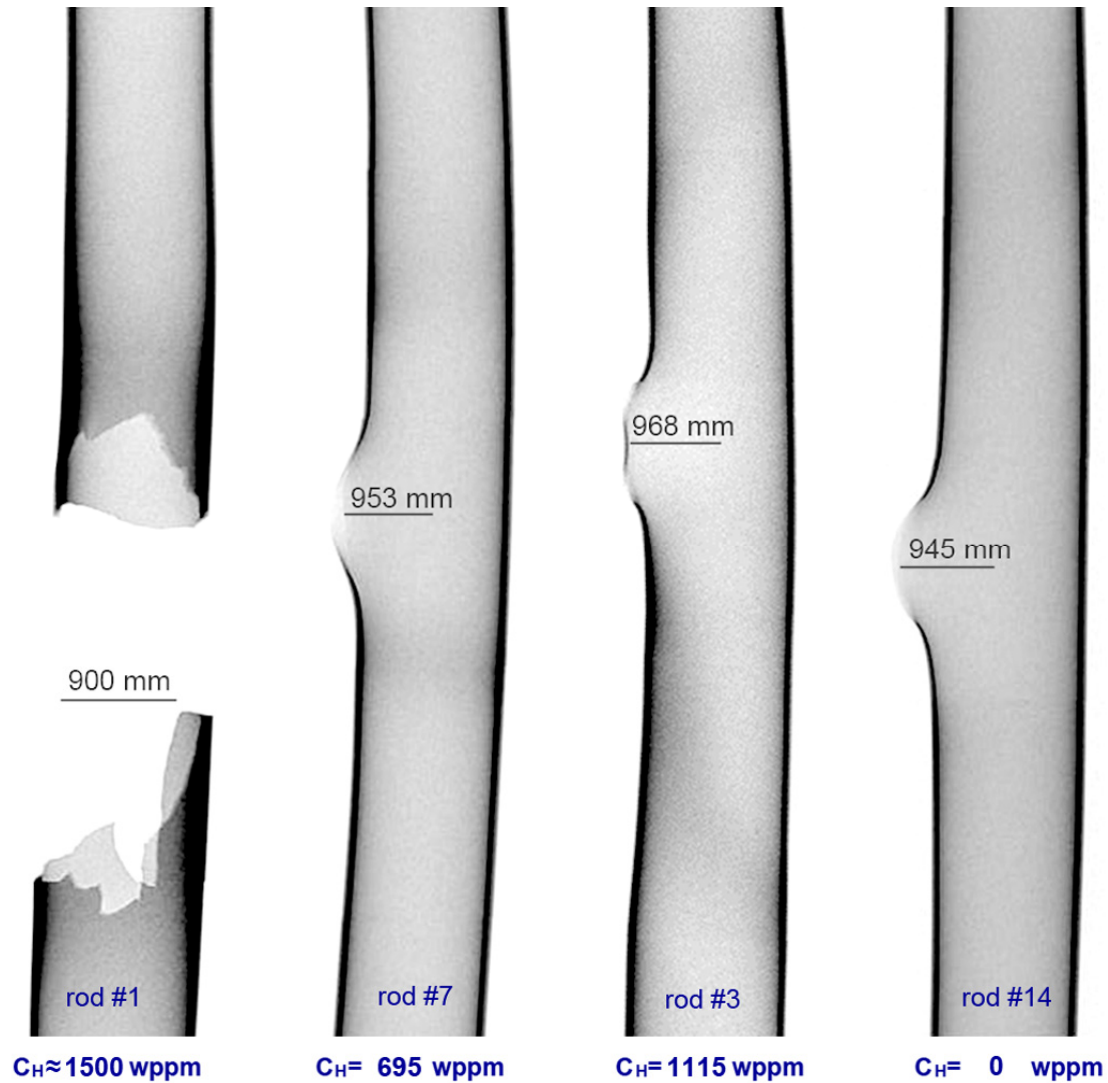
Secondary hydriding QL0: hydrogen bands around burst location (with quantitative results of n⁰-tomography)



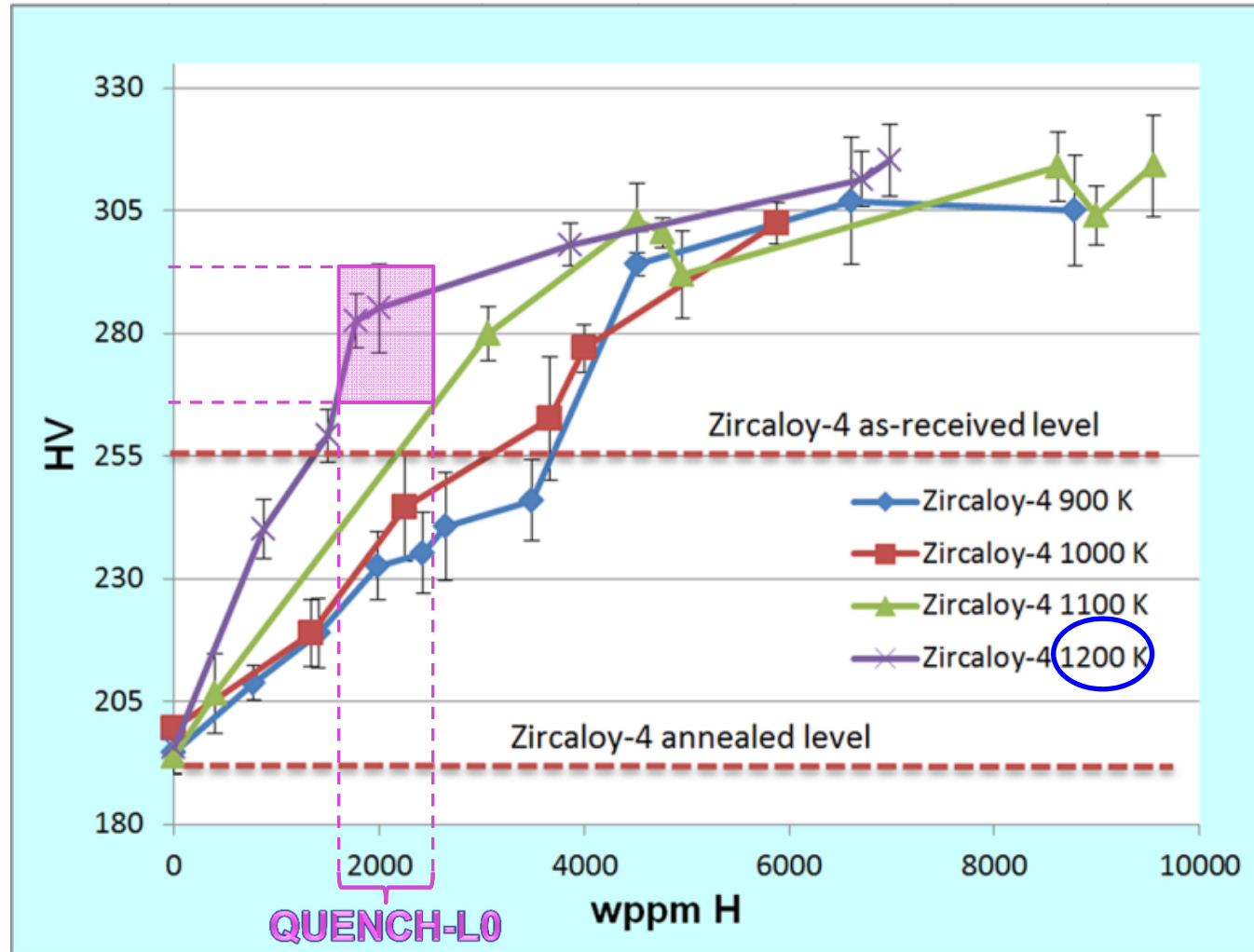
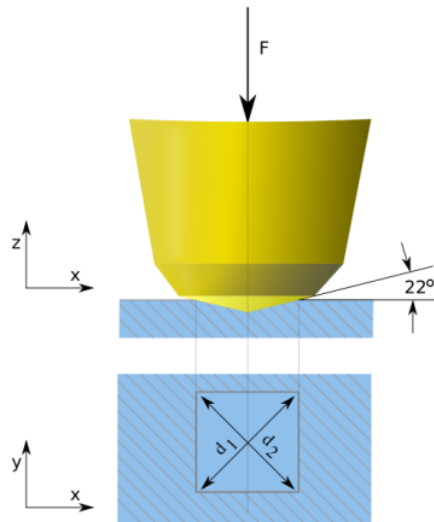
rods #7 and #14:
tube ruptures during
tensile testing
at room temperature

Secondary hydriding QL1: hydrogen bands around burst location (with quantitative results of n⁰-tomography)

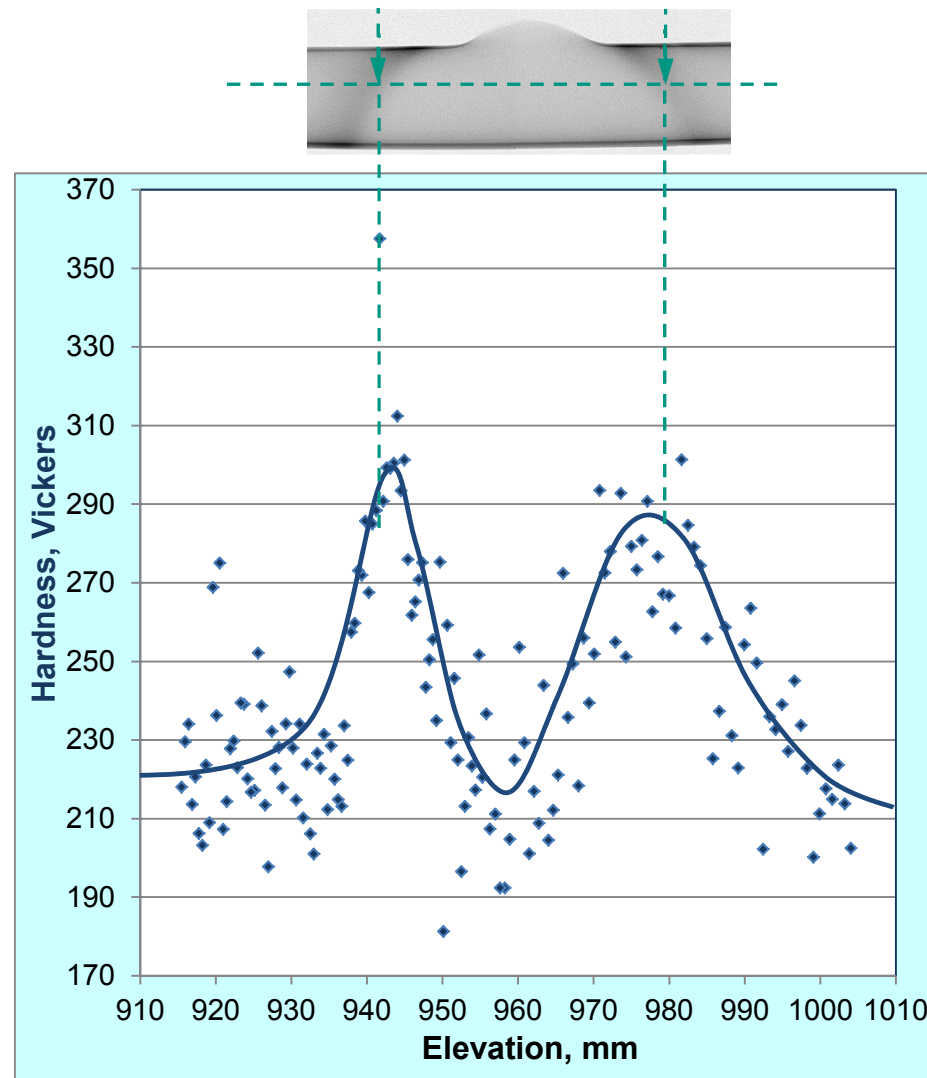
rod #1:
tube failure during
dismantling of the bundle
at room temperature



Micro hardness (Vickers) of hydrated single samples: dependence on hydrogen content and temperature



QUENCH-L0 test: microhardness peaks at hydrogen bands

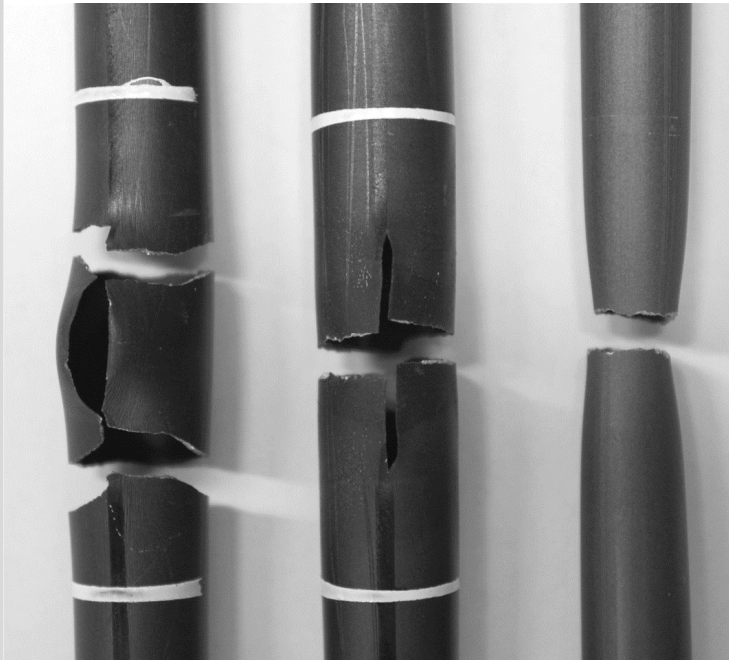


rod #3; $t_{burst} = 119$ s; $T_{burst} = 820^{\circ}\text{C}$; $A_{burst} = 40$ mm²

Failure behavior during tensile tests at room temperature

QL0: 3 types

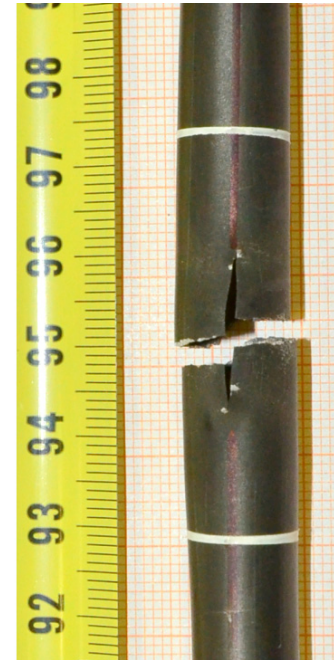
QL1: only stress concentration
(excepted rod #1 brittle ruptured during handling)



hydrogen embrittlement (inner rods with $C_H > 1500$ wppm)
 stress concentration (outer rods with $C_H > 1000$ wppm)
 necking (outer rods)



rod #4
 $C_H = 730$ wppm



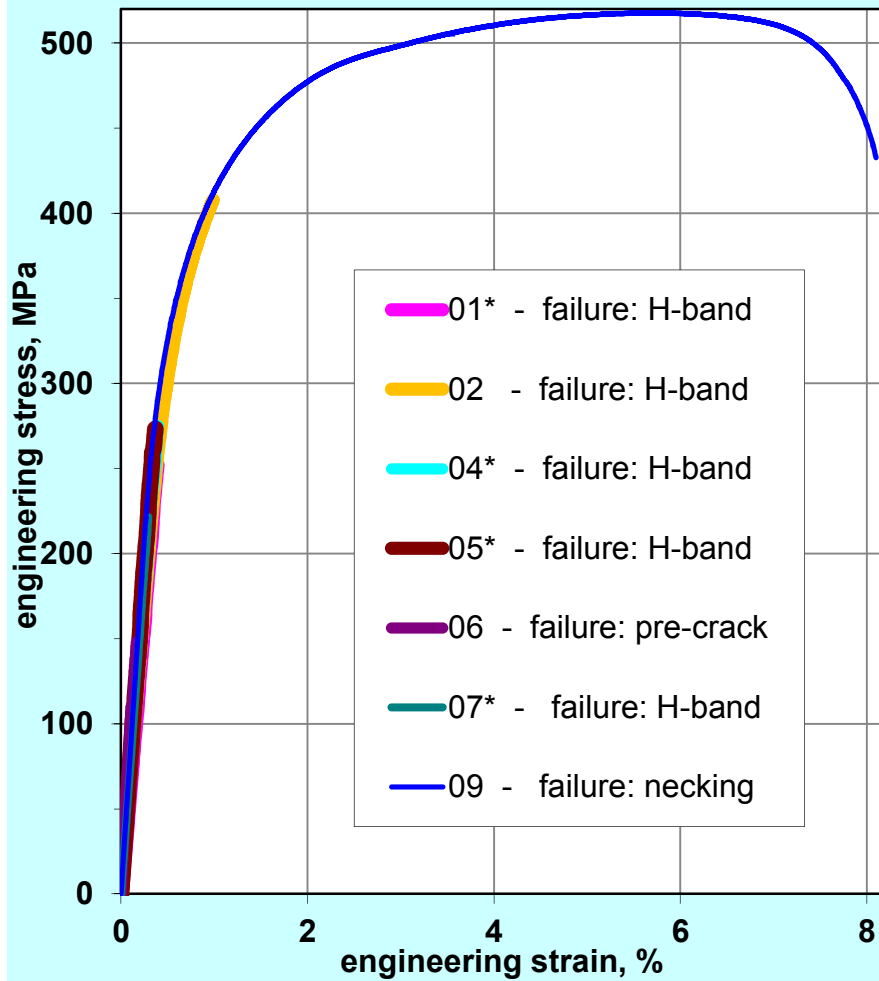
rod #6
 $C_H = 795$ wppm



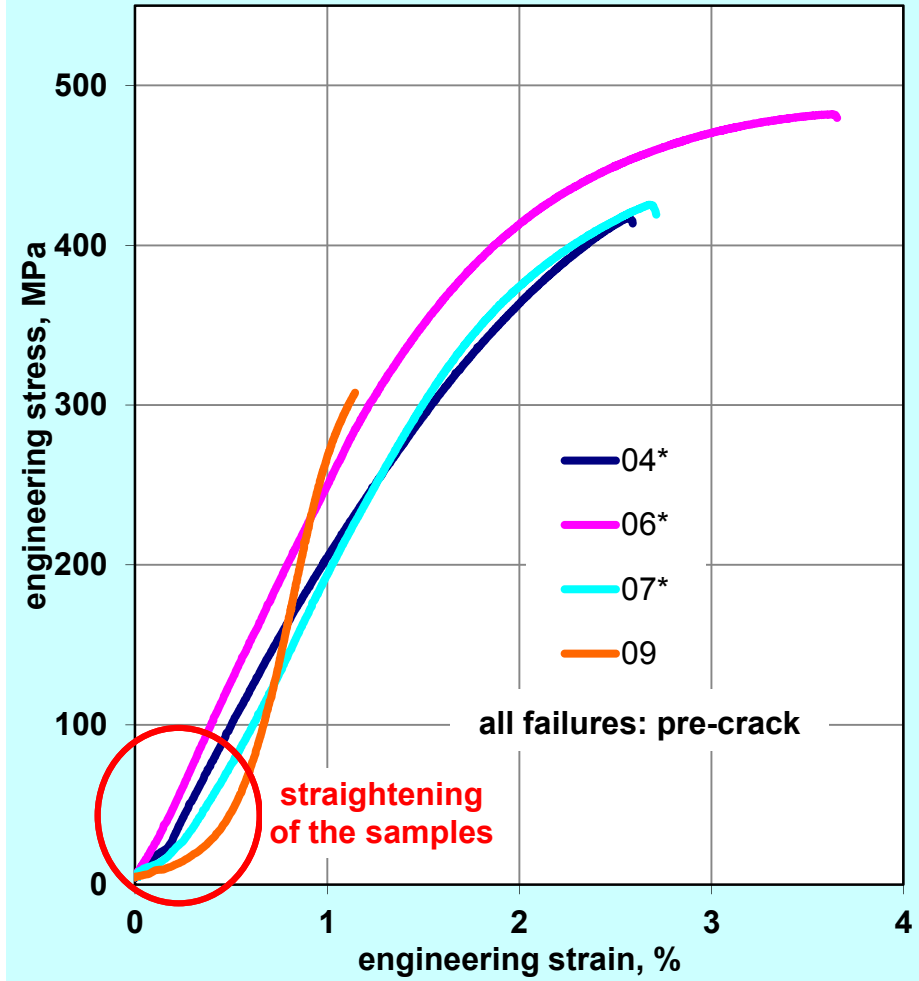
rod #9
 $C_H = 1270$ wppm

Tensile tests for inner rods

QL0 sample length 500 mm or 250 mm*



QL1 sample length 1000 mm or 250 mm*



Results of tensile tests

QL0

rod l ₀ =500 mm *l ₀ =250 mm	ultimate tensile strength [MPa]	fracture stress [MPa]	elongation at fracture [%]	rupture based on:
01*	254	254	0.38	hydrogen embrittlement
02	408	408	0.99	hydrogen embrittlement
04*	276	276	0.40	hydrogen embrittlement
05*	274	274	0.37	hydrogen embrittlement
06	148	148	0.16	stress concentration
07*	222	222	0.29	hydrogen embrittlement
09	518	433	8.10	necking
10	512	507	10.12	necking
11	509	391	11.67	necking
12	502	499	6.44	stress concentration
13	504	504	9.18	stress concentration
14	430	430	1.97	stress concentration
15	505	450	11.70	necking
16	512	389	10.95	necking
17	501	497	3.83	failure at stuck pellet
18	513	458	10.19	necking
19	489	368	11.80	necking
20	452	447	2.20	stress concentration
21	506	498	8.11	stress concentration

QL1

rod l ₀ =1000 mm *l ₀ = 250 mm	ultimate tensile strength [MPa]	fracture stress [MPa]	elongation at fracture (graded) [%]	rupture based on:
04*	416	414	0.75 (0.68)	stress concentration
06*	499	481	1.70 (1.68)	stress concentration
07*	436	425	1.03 (0.81)	stress concentration
09	307	307	0.59 (0.09)	stress concentration
12	464	464	5.50 (5.27)	stress concentration
13	518	515	5.13 (5.03)	stress concentration
14	471	471	3.96 (3.80)	stress concentration
16	462	456	4.31 (4.10)	stress concentration
17*	333	327	0.33 (0.33)	stress concentration
18*	270	263	0.19 (0.19)	stress concentration
20*	367	356	1.13 (1.06)	stress concentration

Summary

- Two out-of-pile bundle tests, QUENCH-L0 and QUENCH-L1, with the same bundle geometry and the same cladding material (Zircaloy-4) were performed under LOCA conditions to investigate the phenomenon of the so-called cladding secondary hydriding. The tests differed in (1) heat-up rate during the first transient (max 2.5 K/s for QL0 and max 7.5 K/s for QL1); (2) absence (QL0) and presence (QL1) of a cool-down phase before quenching.
- The cladding burst occurred at temperatures between 1123 and 1223 K for QL0 and between 1073 and 1173 K for QL1 (i.e. in both cases the burst temperatures were inside the temperature region corresponding the $\alpha \rightarrow \alpha + \beta \rightarrow \beta$ phase transition of the Zircaloy-4 alloy).

Summary (cont.)

- Post-burst duration of inner cladding oxidation at high temperatures was shorter in case of the more prototypical test QL1. Correspondingly, the amount of hydrogen absorbed by claddings close to their burst openings was lower for the QL1 (less than 1700 wppm) than for QL0 (less than 2600 wppm).
- Tensile tests at room temperature with claddings of both bundles showed that claddings with hydrogen contents *less than 1500 wppm* ruptured inside the burst opening due to *stress concentration*, whereas claddings with hydrogen contents *more than 1500 wppm* fractured *along the hydrogen bands*.

Acknowledgment

The QUENCH-LOCA experiments are supported and partly sponsored by VGB PowerTech e.V., Essen, Germany, European technical association for power and heat generation.

The authors would like to thank Mr. J. Moch, Dr. H. Leiste, Mrs. J. Laier and Mrs. U. Peters for intensive work during test preparation and post-test investigations

Thank you for your attention

<https://www.iam.kit.edu/wpt/loca/>
<http://www.iam.kit.edu/wpt/471.php>
<http://quench.forschung.kit.edu/>